Studies of the Ethanol-Induced Interdigitated Gel Phase in Phosphatidylcholines Using the Fluorophore 1,6-Diphenyl-1,3,5-hexatriene†

Parthasarathy Nambi,‡,‖ Elizabeth S. Rowe,*,‡ and Thomas J. McIntosh§

University of Kansas Medical Center, Kansas City, Kansas 66103, Veterans Administration Medical Center, Kansas City, Missouri 64128, and Department of Anatomy, Duke University Medical Center, Durham, North Carolina 27710

Received February 29, 1988; Revised Manuscript Received July 18, 1988

ABSTRACT: It is now well established that a number of amphiphilic molecules such as ethanol can induce the formation of the fully interdigitated gel phase in phosphatidylcholines. We have shown earlier that alcohols such as ethanol induce biphasic melting behavior in phosphatidylcholines [Rowe, E. S. (1983) *Biochemistry 22*, 3299–3305] but not in phosphatidylethanolamines [Rowe, E. S. (1985) *Biochim. Biophys. Acta 813*, 321–330]. Simon and McIntosh [(1984) *Biochim. Biophys. Acta 773*, 169–172] showed that the alcohol-induced biphasic melting behavior in phosphatidylcholines is a consequence of acyl chain interdigitation. In the present study we demonstrate the detection of the transition of DPPC and DSPC to the interdigitated phase in the presence of ethanol using the fluorescence properties of the commonly used fluorophore 1,6-diphenyl-1,3,5-hexatriene (DPH). By correlating fluorescence and X-ray diffraction results, we have demonstrated the use of fluorescence to study the phase transition from the noninterdigitated to the interdigitated phase. Using this method, we have investigated the temperature and ethanol concentration dependence of the induction of the interdigitated phase in DSPC and DPPC and shown that the induction of interdigitation by ethanol is temperature dependent, with higher temperature favoring interdigitation. The temperature–ethanol phase diagrams have been determined for DPPC and DSPC.

It is now recognized that saturated symmetrical and asymmetrical phosphatidylcholines (PC's)[1] can exist in an unusual gel phase in which the acyl chains from opposing monolayers interdigitate (Xu & Huang, 1987; Simon & McIntosh, 1984; McDaniel et al., 1983; McIntosh et al., 1983, 1984; Cunningham & Lis, 1986; Cunningham et al, 1986; Ruocco et al., 1985; Serrallach et al., 1983; Huang et al., 1983; Hui et al., 1984; Mattai et al., 1987; Hui & Huang, 1986). The existence of the interdigitated phase ($L_\beta I$) has been demonstrated in a number of like chain PC's under a variety of conditions. For example, substances such as glycerol, methanol, ethylene glycol, benzyl alcohol, chlorpromazine, tetracaine (McDaniel et al., 1983; McIntosh et al., 1983), ethanol (Simon & McIntosh, 1984), and thiocyanate ion (Cunningham & Lis, 1986) can induce the formation of $L_\beta I$ in PC's. The interdigitated gel phase has also been observed in the absence of any inducer in dihexadecylphosphatidylcholine (DHPC) (Ruocco et al., 1985; Laggner et al., 1987; Kim et al., 1987), in β-DPPC (Serrallach et al., 1983), and in DPPC and DSPC under hydrostatic pressure (Braganza & Worcester, 1986).

We have been interested in the interaction of alcohols with synthetic model membranes (Rowe, 1983, 1985, 1987; Rowe et al., 1987a; Veiro et al., 1987, 1988; Herold et al., 1987). We have shown that short-chain alcohols induce a biphasic melting behavior in PC's (Rowe, 1983, 1985); that is, the main transition temperature of PC's is reduced at low concentrations of alcohol but increased at high concentrations. It was shown that the longer the acyl chain length of the lipid, the lower the alcohol concentration at which the inflection in T_m occurs (Rowe, 1983). It was subsequently shown by Simon and McIntosh (1984) that the alcohol-induced biphasic behavior observed in PC's is a consequence of acyl chain interdigitation. In contrast, the phosphatidylethanolamines (PE's) do not exhibit similar biphasic melting behavior in the presence of alcohols, implying that PE's do not form the interdigitated gel phase under comparable conditions (Rowe, 1985).

Biphasic behavior in the melting transition has been observed in PC's in the presence of a number of compounds which are known from X-ray diffraction to induce interdigitation (Rowe et al., 1987b). These observations are indications of the differential interactions of the normal bilayer gel and the interdigitated gel with the inducers. Recently, we have shown that ethanol can induce lateral phase separations in PC–PE mixtures, in which both interdigitated and noninterdigitated regions apparently coexist (Rowe, 1987). In addition, we have recently demonstrated that alcohols decrease the pretransition temperature of PC's, with the effectiveness of the alcohol increasing with alcohol chain length (Veiro et al., 1987).

The threshold alcohol concentration for the inflection in the main transition temperatures of PC's, which is an indirect indicator of the induction of the $L_\beta I$ phase, was found to decrease with increasing acyl chain length (Rowe, 1983). However, since the main transition temperature increases with

† This work was supported by the Medical Research Service of the Veterans Administration and by a grant from the National Institute of Alcohol Abuse and Alcoholism (AA 05371) to E.S.R. and by a grant from the National Institutes of Health (GM 27278) to T.J.M.

* Address correspondence to this author at Research Services, Veterans Administration Medical Center, 4801 Linwood Blvd., Kansas City, MO 64128.

‡ University of Kansas Medical Center and Veterans Administration Medical Center.

‖ Present address: Chemistry Department, Mercer University, Macon, GA 31207.

§ Duke University Medical Center.

[1] Abbreviations: PC, phosphatidylcholine; DPPC, 1,2-dipalmitoylphosphatidylcholine; DSPC, 1,2-distearoylphosphatidylcholine; DPH, 1,6-diphenyl-1,3,5-hexatriene; DPHPC, 1-palmitoyl-2-[3-(1,3,5-hexatrienyl)propanoyl]phosphatidylcholine; PE, phosphatidylethanolamine; β-DPPC, 1,3-dipalmitoylphosphatidylcholine; DHPC, 1,2-dihexadecyl-*sn*-glycero-3-phosphocholine; Lc, crystalline bilayer phase; $L_{\beta'}$, tilted chain bilayer gel phase; $P_{\beta'}$, rippled gel phase; L_α, liquid-crystalline bilayer phase; $L_\beta I$, interdigitated gel phase.

0006-2960/88/0427-9175$01.50/0

increasing acyl chain length, it could not be determined whether the observed effect was due to the chain length of the lipid or to a temperature effect on the alcohol–lipid interactions.

One of the difficulties in studying the transition of PC's among the various gel phases is that it is difficult to detect the transition from the noninterdigitated gel to the interdigitated gel. We have previously used the indirect means of detecting the transition of the gel to the interdigitated phase by observing its effects on the main transition and pretransition (Rowe et al., 1987b). In the current investigation we report the development of a fluorescence method using 1,6-diphenyl-1,3,5-hexatriene (DPH) to directly detect the transition from the bilayer gel to the interdigitated gel. The method is validated by direct X-ray diffraction measurements. Using this method, we have studied the effect of temperature and alcohol concentration on the transition of DPPC and DSPC to the interdigitated phase. The results obtained are used to determine the temperature–ethanol phase diagrams for DSPC and DPPC.

Materials and Methods

Materials. The lipids were from either Avanti Polar Lipids, Birmingham, AL, or Sigma Chemical Co., St. Louis, MO, and were used as received. The purity of the lipids was checked by thin-layer chromatography. The fluorophores, DPH and DPHPC, were obtained from Molecular Probes, Eugene, OR. Ethanol ("200" proof) was obtained from Publicker Industries Co., Linfield, PA.

Samples. The stock solution of the lipids and the probes was prepared in chloroform; the lipid concentration of the stock solution was 1.3 mM. The chloroform stock solutions of the lipid and the probe were kept in the freezer until ready to use. Appropriate volumes of the chloroform solution of the lipid and the probe were mixed to give a lipid to probe ratio of 500 to 1. This probe concentration is well below that which alters the lipid properties (Lentz et al., 1976). Chloroform was removed by first using N_2 gas and removing the final residual chloroform under vacuum. Double-distilled water was added to the thin film containing the lipid and the probe. Nitrogen was bubbled to remove any dissolved oxygen, and the lipid was hydrated at about 10 °C above the chain melting temperature of the lipid for at least 1 h. During this incubation, the sample was vortexed periodically. The concentration of lipid for the fluorescence experiments was 0.13 mM.

Fluorescence. The fluorescence experiments were performed on the SLM 8225 spectrofluorometer interfaced to an Apple IIe; methodology was as described previously (Veiro et al., 1987). The excitation wavelength was 351 nm, and the emission spectra were measured from 380 to 560 nm. High-pass cutoff filters were used to minimize the scattered light. The lipid concentration was kept low in order to minimize the scattering contributions from the sample. Experiments without the probe showed that the signal from stray scattered light was less than 2% of the signal from the samples with the probe at the same lipid concentration. The extent of apparent fluorescence quenching was determined from the integrated values of the emission spectra. The integration was performed with a software routine provided by SLM. Titration experiments were performed at constant temperature by adding the desired amount of ethanol and incubating for 15 min before measuring the emission spectrum. After corrections for the dilution effects were made, the data were plotted in a pseudo-Stern–Volmer form in which the ratio F_0/F (where F_0 is the value of the integrated intensity in the absence of alcohol and F is the value in the presence of alcohol) was plotted against the concentration of ethanol. For the temperature scans at constant alcohol concentration, the fluorescence emission was monitored at 430 nm, and the temperature was controlled by water circulating from an external programmable bath. The rate of heating was 1 °C/min.

The fluorescence lifetime measurements were made on the SLM 4800 fluorometer. The measurements were made at 25 °C with two frequencies, 30 and 6 mHz. The fluorophore 1,4-bis(4-methyl-5-phenyloxazol-2-yl)benzene (Me_2POPOP) was used as the reference, and its lifetime in absolute ethanol was assumed to be 1.45 ns (Lakowicz, 1983). Heterogeneity analysis was performed by the method of Weber (1981), with the data obtained at two frequencies, 6 and 30 mHz. For each measurement the major component represented at least 95% of the fluorescence, with a minor component having a lifetime near 1 ns. The results are reported in the text as the lifetime of the major component.

X-ray Diffraction. For X-ray diffraction experiments, multilamellar suspensions (10 mg/mL) were concentrated by a brief (10-min) spin with a bench centrifuge and then sealed in quartz glass X-ray capillary tubes. The capillary tubes were mounted in a temperature-regulated specimen holder in a pinhole collimation X-ray camera containing three sheets of Kodak DEF 5 direct exposure X-ray film in a flat-plate film cassette. X-rays were produced by a Jarrell–Ash microfocus X-ray unit operated at 40 kV and 6 mA. The specimen-to-film distance was 10 cm, and exposure times were on the order of 5–10 h. Films were processed by standard techniques and analyzed with a Joyce–Loebl microdensitometer, Model MKIIIC. Densitometer scans were taken in a radial direction across the film. The background curve was subtracted, and integrated intensities $I(h)$, where h is the diffraction order, were obtained as previously described (McIntosh, 1980). For these unoriented specimens, the structure amplitude for order h was set equal to $[h^2I(h)]^{1/2}$. Electron density profiles were calculated by the formula

$$\rho(x) = \sum\phi(h)[h^2I(h)]^{1/2}\cos(2\pi xh/d)$$

where d is the lamellar repeat period and $\phi(h)$ is the phase angle for each order h. The same phase angles were used as previously determined (McIntosh, 1978; McIntosh et al., 1983) for the gel ($L_{\beta'}$) and interdigitated ($L_{\beta}I$) phases of DPPC.

Results

The fluorescence emission spectra of DPH in DPPC vesicles measured at 25.2 °C at different ethanol concentrations are shown in Figure 1. It is seen that the fluorescence intensity of DPH in DPPC vesicles is reduced as the concentration of ethanol is increased. Similar results were also obtained with DSPC vesicles containing DPH in the presence of ethanol (data not shown).

The change in DPH fluorescence in DPPC vesicles by ethanol is plotted as F_0/F against ethanol concentration in Figure 2, where F_0 and F are the integrated intensities in the absence of ethanol and in the presence of the given ethanol concentration, respectively, determined from spectra such as shown in Figure 1. This plot shows that the reduction in intensity appears in a sigmoidal fashion over a narrow concentration of ethanol, with a maximum reduction of over 50% of the original intensity. Also shown in Figure 2 is a similar experiment using the PC-linked DPH probe DPHPC. This probe exhibits only a small degree of apparent quenching, which occurs as a function of ethanol concentration. In view of the comparison of these two probes, DPH was chosen as the probe for pursuing these experiments. Fluorescence lifetime measurements were performed as described under Ma-

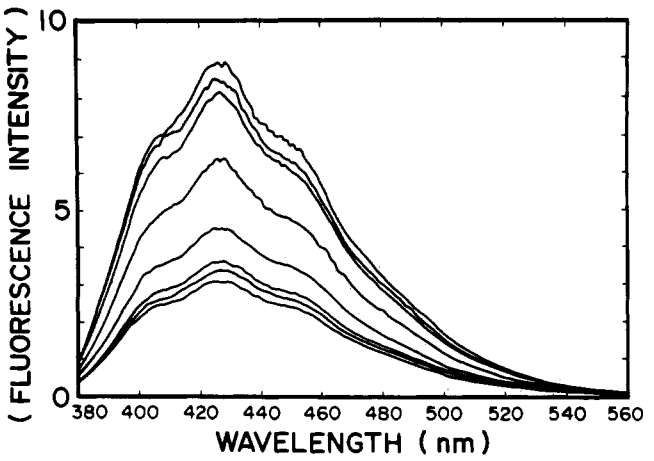

FIGURE 1: Emission spectra of DPH in DPPC vesicles measured at 25 °C in the presence of different concentrations of ethanol. Curves numbered from the top down: (1) 0.0 M; (2) 0.22 M; (3) 0.65 M; (4) 1.09 M; (5) 1.30 M; (6) 1.74 M; (7) 1.96 M; (8) 2.61 M.

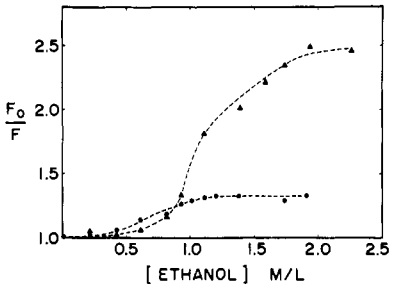

FIGURE 2: Comparison of the ethanol-induced apparent quenching in DPH- and DPHPC-labeled DPPC vesicles. $T = 25$ °C. Triangles, DPH; circles, DPHPC.

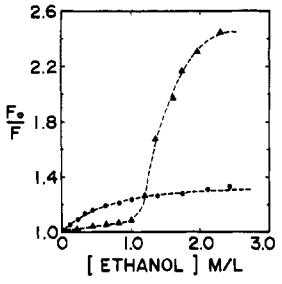

FIGURE 3: Comparison of the apparent quenching of DPH as a function of ethanol concentration in the gel at 20.7 °C (triangles) and the liquid-crystalline phase at 45.0 °C (circles).

terials and Methods for DPH-containing vesicles in aqueous suspension in the presence and absence of ethanol. The values obtained were 9.61 ns in the absence of ethanol and 9.55 ns in the presence of 1.2 M ethanol. These are the same within experimental error and are similar to those found in the literature for DPH in gel-phase PC vesicles (Barrow & Lentz, 1985).

A comparison of the apparent DPH quenching in DPPC in the gel and liquid-crystal phases by ethanol is shown in Figure 3. The reduction of DPH fluorescence in the gel phase, measured at 20 °C, appears over a narrow concentration range with a midpoint at 1.2 M ethanol. In contrast, in the liquid-crystal phase at 45 °C, a similar ethanol titration experiment gives a nearly linear small quenching effect, as expected for a system in which there is no expected phase change in the lipid. The sigmoidal nature of the apparent quenching curve in the gel phase, and the large magnitude of the change, suggests a cooperative change in the environment of the fluorophore, since quenching itself as a solvent perturbation

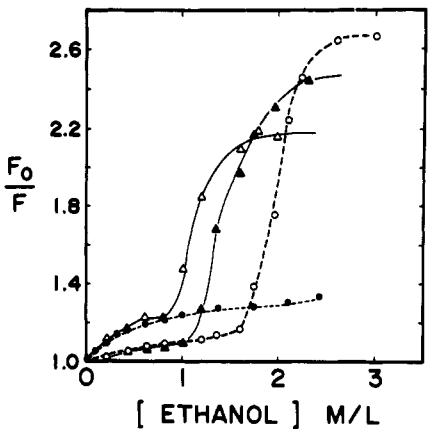

FIGURE 4: Effect of temperature on the apparent quenching of DPH in DPPC vesicles as a function of ethanol. Open triangles, 30.4 °C; closed triangles, 20.7 °C; open circles, 11.0 °C; closed circles, 45.0 °C.

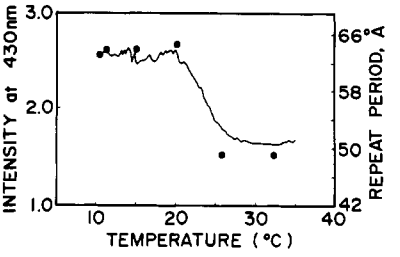

FIGURE 5: Effect of temperature on the fluorescence intensity of DPH at 430 nm (solid line) and lamellar repeat period of DPPC in the presence of 1.2 M ethanol (closed circles).

would be expected to be linear. It is well established that DPPC undergoes a gel to gel transition from the noninterdigitated to the interdigitated gel at 20 °C between 0.8 and 1.3 M ethanol (Simon & McIntosh, 1984). This suggests that the sigmoidal curve shown in Figure 3 for DPPC as a function of ethanol concentration at 20 °C is a result of the L_{β}' to $L_{\beta}I$ transition. Direct evidence for this conclusion from X-ray diffraction measurements is provided below. Thus, DPH fluorescence intensity measurements can be used to monitor the L_{β}' to $L_{\beta}I$ transition.

DPH fluorescence intensity measurements were used to study the temperature dependence of the induction of the $L_{\beta}I$ phase by ethanol. Figure 4 shows apparent DPH quenching as a function of ethanol concentration at four temperatures for DPPC. At the lower temperature (11 °C) ethanol concentrations greater than 1.6 M were needed to induce the sigmoidal transition, compared to 1.2 M at 20 °C. Thus, it appears that the ethanol-induced L_{β}' to $L_{\beta}I$ transition is temperature dependent, with higher temperature favoring the $L_{\beta}I$ phase. The curve at 30 °C shows a small increase in apparent quenching below 0.5 M ethanol, with the major sigmoidal change occurring at 0.8 M ethanol. The minor change is apparently due to the pretransition (L_{β}' to P_{β}') of DPPC, which has been shown to occur at 30 °C at 0.5 M ethanol (Veiro et al., 1987). It is also seen in Figure 4 that the final extent of quenching depends on the temperature; the explanation for this effect is not apparent.

The results shown in Figure 4 demonstrate that the L_{β}' to $L_{\beta}I$ transition is temperature dependent, making it possible to study the transition by scanning the temperature at constant ethanol concentration. Figure 5 shows the fluorescence intensity at 430 nm of DPH-labeled DPPC as a function of temperature in the presence of 1.2 M ethanol. There is a sigmoidal reduction in intensity observed with a midpoint at 25 °C. This is consistent with the results presented in Figure

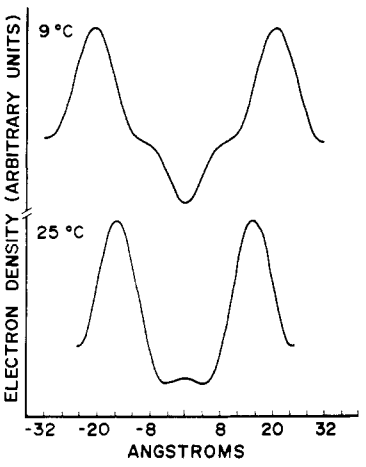

FIGURE 6: Electron density profile of DPPC with 1.2 M ethanol at (A) 9 and (B) 25 °C.

4 as a function of alcohol concentration, demonstrating that the L_{β}' to $L_{\beta}I$ transition is induced by heating.

In order to establish that the transition seen in Figure 5 is indeed the L_{β}' to $L_{\beta}I$ transition, X-ray diffraction measurements of DPPC suspensions in 1.2 M ethanol were made as a function of temperature. For temperatures between 9 and 15 °C, the X-ray patterns consist of 5 orders of a lamellar repeat period of 63 Å and two wide-angle reflections—a sharp reflection at 4.20 Å and a broad band centered at 4.09 Å. These patterns are characteristic of the gel (L_{β}') phase of DPPC (Tardieu et al., 1973; McIntosh, 1980). For temperatures of 25 and 32 °C, the diffraction pattern consists of 3 orders of a lamellar repeat period of 49 Å and a single sharp wide-angle reflection at 4.10 Å. These patterns are characteristic of DPPC in the interdigitated ($L_{\beta}I$) phase (Ranck et al., 1977; McIntosh et al., 1983; Simon & McIntosh, 1984). At 20 °C, the X-ray pattern contains the 5 lamellar orders of the 63-Å repeat period, plus a very weak reflection at 49 Å, which indicates that this temperature is near the transition between the two phases. The measured lamellar repeat periods as a function of temperature are plotted in Figure 5, along with the fluorescence intensity measured at the same alcohol concentration. This figure shows that the structural change determined by X-ray diffraction occurs at the same temperature as the transition observed by fluorescence intensity.

Calculated electron density profiles of DPPC in 1.2 M/L ethanol at 9 and 25 °C are shown in Figure 6. Structure factors used in these calculations are as follows: $F(1) = -5.36$, $F(2) = -4.70$, $F(3) = +2.87$, $F(4) = -1.66$, and $F(5) = -1.13$ for the profile at 9 °C; $F(1) = -4.52$, $F(2) = -4.26$, and $F(3) = +3.21$ for the profile at 25 °C. In both profiles the geometric center of the bilayer is located at the origin (0 Å), and the two highest density peaks (located at ±21 Å for the profile at 9 °C and at ±15 Å for the profile at 25 °C) correspond to the lipid headgroups. The deep trough located at 0 Å in the profile at 9 °C corresponds to the localization of the low-density terminal methyl groups in the bilayer in the L_{β}' phase. This central trough is absent in the profile at 25 °C. Both the decrease in headgroup separation across the bilayer and the loss of the terminal methyl trough in the center of the profile are consequences of the lipid chain interpenetration or interdigitation (Ranck et al., 1977; McIntosh et al., 1983). Model calculations based on profiles similar to those shown in Figure 6 indicate that in the $L_{\beta}I$ phase the hydrocarbon chains of one monolayer interpenetrate up to the first or second methylene group of the chains of the opposing monolayer (McIntosh et al., 1983).

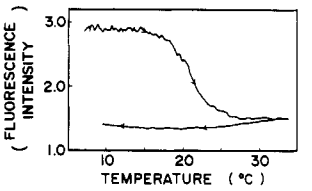

FIGURE 7: Effect of temperature on the fluorescence intensity of DPH in DPPC vesicles with 1.4 M added ethanol, for a heating scan followed by a cooling scan. Arrows indicate the direction of the scan. Scan rate, 1.0 °C/min.

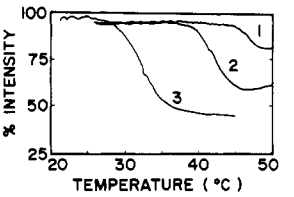

FIGURE 8: Effect of ethanol concentration on the fluorescence intensity of DPH in DSPC vesicles for different ethanol concentrations: (1) 0.44 M; (2) 0.60 M; (3) 0.80 M.

The thermal reversibility of the L_{β}' to $L_{\beta}I$ transition was examined by measuring the fluorescence intensity of DPH at 430 nm in the presence of 1.4 M ethanol for heating and cooling scans as shown in Figure 7. It appears that the L_{β}' to $L_{\beta}I$ transition is thermally irreversible. However, it was found that after incubation of the sample overnight at low temperature the heating transition was restored, suggesting that the reverse reaction is very slow.

The role of the acyl chain length in the L_{β}' to $L_{\beta}I$ transition was investigated by examining DSPC in the presence of ethanol with DPH fluorescence intensity measurements. The fluorescence intensity of DPH in DSPC was measured as a function of temperature in the presence of various ethanol concentrations; some of the representative transition curves are shown in Figure 8. Curve 3, at 0.8 M ethanol, exhibits a reduction of DPH fluorescence of 50%, similar to that observed in DPPC for the L_{β}' to $L_{\beta}I$ transition. In contrast, at 0.44 M ethanol there is a transition observed at 47 °C which gives a reduction of intensity of about 10%. A similar small apparent quenching transition was observed in the absence of ethanol (data not shown). The transition observed in curve 1 at 0.44 M ethanol corresponds to the pretransition (L_{β}' to P_{β}') previously studied by spectrophotometry (Veiro et al., 1987; Veiro, unpublished results). Curve 2 in Figure 8 represents the fluorescence intensity at 0.6 M ethanol. It gives an intermediate degree of apparent quenching; however, there is no indication of multiple transitions. Similar results were obtained with DPPC.

Figure 9 shows the percent fluorescence decrease for the total transition for temperature scans of DSPC performed at different ethanol concentrations. The transition temperature for each heating scan is also plotted as a function of ethanol concentration. It is evident that there is sharp increase in the percent quenching that occurs with a midpoint at about 0.62 M ethanol. The open circles, representing the transition temperatures of the "low quenching" transitions, agree with the temperature dependence of the pretransition as previously measured by spectrophotometry (Veiro et al., 1987). The midpoint of the percent apparent quenching curve occurs at the same ethanol concentration at which the pretransition (L_{β}' to P_{β}') observed by optical density disappears (Veiro et al., 1987; Veiro, unpublished results). Thus, it may be concluded that the change in magnitude of the apparent quenching represents the replacement of the L_{β}' to P_{β}' transition with the

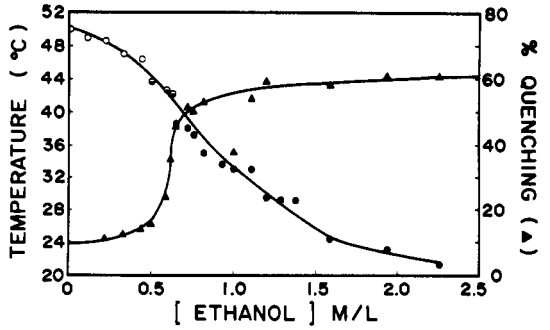

FIGURE 9: Magnitude of fluorescence intensity reduction for DSPC transition as a function of ethanol concentration. Also shown is the transition temperature for the observed transition. Data obtained by temperature scans at fixed ethanol concentration, such as shown in Figure 8. Triangles represent the total percent apparent quenching for the transition at each ethanol concentration. Circles represent the transition temperature. On the basis of the magnitude of quenching, the open circles represent the pretransition (L_{β}' to P_{β}') and the closed circles represent the L_{β}' to $L_{\beta}I$ transition; half-filled circles represent transitions with intermediate magnitudes of apparent quenching.

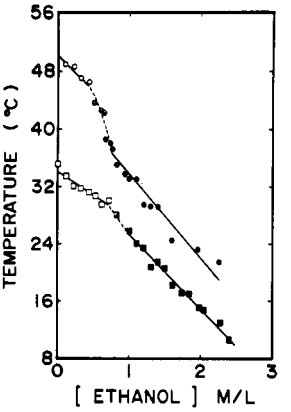

FIGURE 10: Effect of ethanol concentration on the transition temperatures for DPPC and DSPC, obtained from temperature scans at constant ethanol concentration such as shown in Figure 8. The upper curve represents data for DSPC from Figure 9; the lower curve represents data for DPPC. As in Figure 9, the open symbols represent the pretransition, assigned by magnitude of quenching, and the closed symbols represent the L_{β}' to $L_{\beta}I$ transition. Half-filled symbols represent transitions with intermediate magnitudes of apparent quenching.

L_{β}' to $L_{\beta}I$ transition as a function of ethanol concentration. In the plot in Figure 9 the L_{β}' to $L_{\beta}I$ (pretransition) temperatures are represented by open circles, and the L_{β}' to $L_{\beta}I$ transition temperatures are represented by closed circles. The scans exhibiting intermediate magnitudes of quenching are represented by half-filled circles.

The threshold ethanol concentration for the biphasic effect of ethanol on the main transition in DSPC is 0.6 M ethanol (Rowe, 1983), similar to the ethanol concentration for the P_{β}' to $L_{\beta}I$ transition indicated in Figure 9. The biphasic effect has been interpreted to be the result of the induction of interdigitation in the gel state (Simon & McIntosh, 1984; Rowe, 1985), i.e., the P_{β}' to $L_{\beta}I$ transition. The agreement between the ethanol concentrations needed for the P_{β}' to $L_{\beta}I$ transition, as indicated in Figure 9, measured at 42 °C, and the threshold ethanol concentration from the biphasic effect on the main transition, measured at 60 °C, indicates that the transition from P_{β}' to $L_{\beta}I$ has little temperature dependence. A similar result was obtained for DPPC.

Figure 10 shows the ethanol concentration dependence of the transition temperature for DPPC and DSPC. Again, the open symbols represent the L_{β}' to P_{β}' transition, and the closed symbols represent the L_{β}' to $L_{\beta}I$ transition as determined by the magnitude of quenching. The temperatures for the pretransition of DPPC and DSPC are in good agreement with those determined previously by spectrophotometry (Veiro et al., 1987; Veiro, unpublished data). It is interesting to note the continuity of the transition temperature for the two transitions as a function of ethanol concentration. For DPPC there a slight change of slope for the L_{β}' to $L_{\beta}I$ transition compared to the L_{β}' to P_{β}' transition. For DSPC there is a more significant change in slope for the alcohol dependence of the two transitions. There was no evidence of multiple transitions occurring at the intermediate alcohol concentrations as a function of temperature for either lipid. This is consistent with the interpretation that the P_{β}' to $L_{\beta}I$ transition is not temperature dependent.

The comparison of the data in Figure 10 for the two lipids shows that the threshold ethanol concentration for the induction of the $L_{\beta}I$ phase is lower for the longer chain lipid. This is consistent with the previous results on the acyl chain dependence of ethanol effects on the main transitions of PC's (Rowe, 1983), in which it was shown that the longer the lipid acyl chains, the lower the alcohol concentration at which the inflection in the melting temperature occurred.

Discussion

Several important findings have resulted from this investigation. First, we have demonstrated the establishment of a fluorescence method which is sensitive to the transitions of PC's between noninterdigitated and interdigitated phases. Second, we have demonstrated that the transition of DPPC and DSPC from the noninterdigitated L_{β}' to the interdigitated $L_{\beta}I$ phase in the presence of ethanol is temperature dependent, with higher temperature favoring the $L_{\beta}I$ phase. And finally, we have constructed the temperature–alcohol phase diagrams for DSPC and DPPC (see below).

Fluorescence Methodology. In this investigation we have demonstrated that the transition of PC from L_{β}' to the fully interdigitated $L_{\beta}I$ phase can be studied by using fluorescence intensity of DPH. The physical methods used to detect and study the interdigitated phase to date include X-ray diffraction (Ranck et al., 1977; McIntosh et al., 1983), infrared and Raman spectroscopy (O'Leary & Levin, 1984), and electron spin resonance (Boggs & Rangaraj, 1985; Boggs et al., 1986). Studies using these methods have been generally focused on the structural characterization of the phases, as opposed to the transitions between this phase and the other lipid-phase states. In much of our previous work we have been restricted to the indirect detection of the interdigitated phase through its effect on the main melting transition characteristics. We have now established by correlating fluorescence and X-ray diffraction data that a significant decrease in DPH fluorescence intensity occurs during the transition of DPPC from the L_{β}' phase to the $L_{\beta}I$ phase. DPH fluorescence intensity measurement now provides a useful and convenient method for studying systematically the conditions under which the transition of PC's to the interdigitated phase takes place.

The fluorescence intensity of DPH is reduced by over 50% as DPPC undergoes the L_{β}' to $L_{\beta}I$ transition (Figures 2–4). The cause of this decrease in fluorescence may be related to a change in the environment of the probe due to a change in location in the membrane that occurs when the lipid undergoes the transition from the noninterdigitated phase to the interdigitated phase. It is believed that DPH is distributed in at least two different ways in the usual bilayer, either in the center of the bilayer oriented parallel to the surface or parallel to the

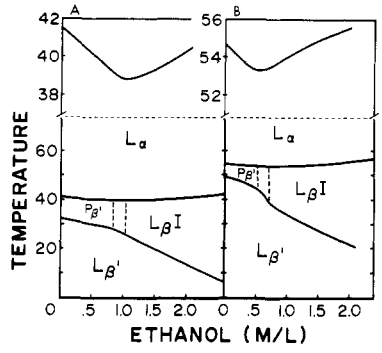

FIGURE 11: Schematic diagram to show the effect of ethanol concentration on phase states for DPPC (A) and DSPC (B). The insets above the diagrams represent an expansion of the temperature scale for the upper curves. Upper curves represent the T_m for the main transition from Rowe (1983), and lower curves represent the data from Figure 10 for the transition midpoints for the $L_{\beta'}$ to $P_{\beta'}$ or $L_{\beta'}$ to $L_\beta I$ transitions.

lipid acyl chains (Davenport, 1985). In the case of the interdigitated phase, it would appear that the orientation parallel to the lipid surface would not be possible, due to the chain penetration across the bilayer center. The phase transition may thus cause the redistribution of the DPH from the center of the bilayer to an orientation parallel to the acyl chains. The change in fluorescence intensity during this change in location in the lipid could be due to a greater exposure of the DPH chromophore to the aqueous solvent due to proximity to the interfacial region of the lipid. The results obtained with the PC-linked DPHPC supports this interpretation, since it exhibits only a very small intensity reduction for this phase transition; due to its linkage to the PC, the DPH moiety is parallel to the acyl chains in either phase. In this case also the apparent quenching effect may be due to an increase in exposure to the aqueous solvent in the interfacial region due to the greater headgroup separation in the $L_\beta I$ phase.

Effect of Temperature on Interdigitation. The most important result of the present study is the finding that the ethanol-induced transition from $L_{\beta'}$ to $L_\beta I$ is strongly temperature dependent, with higher temperature favoring the interdigitated phase. Thus the $L_{\beta'}$ to $L_\beta I$ transition can be induced either by increasing the temperature at constant alcohol concentration or by adding ethanol at constant temperature. Our results on the thermotropic behavior of DSPC and DPPC as a function of the two variables, ethanol concentration and temperature, are summarized in Figure 11, parts A and B. The upper curves represent the effect of ethanol on the main transition of these lipids from Rowe (1983). As seen in the insets with expanded temperature scales above the main phase diagrams, ethanol has a biphasic effect on the main transition. The inflection in T_m has been interpreted as indicative of the transition of the gel phase from the usual gel phase to the interdigitated phase (Simon & McIntosh, 1984; Rowe, 1985; Simon et al., 1986). The lower curves in Figure 11 represent the fluorescence data from Figure 10. The dashed lines connect the threshold region for the biphasic effect on the upper curve (i.e., $P_{\beta'}$ to $L_\beta I$) with the region on the lower curve where the $L_\beta I$ is induced as determined by fluorescence intensity measurements.

The effect of temperature on the transition from $L_{\beta'}$ to $L_\beta I$ must be the result of the combined effects of temperature on one or more of the several factors which lead to the existence of the $L_\beta I$ phase. The major structural changes in going from $L_{\beta'}$ to $L_\beta I$ are the exposure of the terminal methyls from the opposing side of the lamella to the solvent in the interfacial region, along with the concomitant increase in area per headgroup, and an increase in the van der Waals' contacts in the acyl chain region due to a change in packing and loss of chain tilt (Simon & McIntosh, 1984). The thermodynamic effect of the exposure of the terminal methyls to solvent may be temperature dependent, as may the equilibrium constants for the ethanol binding to either phase. The direct effect of temperature on the molecular motions may also be a factor in the temperature-induced $L_{\beta'}$ to $L_\beta I$ transition.

Figure 11 shows that for both lipids the boundary of the region of existence of $L_{\beta'}$ is continuously depressed as a function of ethanol concentration, but the identity of the phase in the adjacent region changes from $P_{\beta'}$ to $L_\beta I$ when the alcohol reaches a threshold concentration. This suggests that the temperature-induced transition from $L_{\beta'}$ to $L_\beta I$ may have underlying causes similar to those which lead to the pretransition ($L_{\beta'}$ to $P_{\beta'}$). In the pretransition, increasing the temperature results in the transition to $P_{\beta'}$, in which the bilayer surface is rippled. This rippling replaces the chain tilt of $L_{\beta'}$ in compensating for the mismatch in area between the choline headgroups and the acyl chains of PC's (Janiak et al., 1976, 1979; Stamatoff et al., 1982). It is apparent in Figure 11 that, above the threshold ethanol concentration, again the $L_{\beta'}$ phase undergoes a transition upon heating, but instead of $P_{\beta'}$ it goes to the interdigitated phase. The structure of this phase, with four acyl chains per headgroup, also solves the mismatch between the areas of the choline groups and the acyl chains and leads to increased mobility in the choline groups (Herold et al., 1987). These considerations suggest that the temperature induction of the $L_{\beta'}$ to $L_\beta I$ transition is due primarily to the effect of temperature on the $L_{\beta'}$ phase.

In contrast to the $L_{\beta'}$ to $L_\beta I$ transition, the $P_{\beta'}$ to $L_\beta I$ transition has little or no temperature dependence. In figure 11, consistent with the phase rule, there are two apparent triple points for both DPPC and DSPC. The first of these points is at the inflection point on the upper curve (0.8 M EtOH, 41 °C for DPPC), where the $P_{\beta'}$, $L_\beta I$, and L_α phases coexist, and there are no degrees of freedom. The second triple point is at the change in slope of the lower curve (0.8 M EtOH, 28 °C for DPPC), where the $L_{\beta'}$, $P_{\beta'}$, and $L_\beta I$ phases coexist, and again there are no degrees of freedom. The triple points in the DSPC diagram are at 0.6 M ethanol, 42 °C, and 0.6 M ethanol, 60 °C. Somewhere between the dashed lines (which delineate the uncertainty) there is a line denoting the $P_{\beta'}$ to $L_\beta I$ transition. The vertical nature of this line, for both DPPC and DSPC, indicates that the $P_{\beta'}$ to $L_\beta I$ transition is independent of temperature and is thus a function of alcohol concentration only. This is consistent with our finding that even at the intermediate alcohol concentrations only one transition was observed by fluorescence intensity in temperature scans.

Alcohol–Lipid Interactions. Several of the features of the diagrams of Figure 11 can be understood in terms of the relative free energies of binding of ethanol for each of the four phases. When ethanol binds preferentially to one phase relative to another, it shifts the equilibrium between the phases toward the phase with the greater binding free energy [see Lee (1977)]. For example, for the main transition ($P_{\beta'}$ to L_α) the greater membrane/buffer partition coefficient of ethanol in L_α relative to $P_{\beta'}$ results in a reduction in T_m as a function of increasing ethanol concentration (Rowe, 1983). Similarly, the negative slope of the boundary between $L_{\beta'}$ and $P_{\beta'}$ indicates that ethanol has preferential interactions with $P_{\beta'}$ relative to $L_{\beta'}$ (Veiro et al., 1987), whereas the positive slope of the boundary between $L_\beta I$ and L_α indicates that $L_\beta I$ has greater affinity for ethanol than L_α (Rowe, 1983; Simon et al., 1986).

It can be deduced from these relationships that the relative order of affinity of ethanol for the four phases is $L_{\beta}' < P_{\beta}' < L_{\alpha} < L_{\beta}I$.

It is likely that both the mechanism of the interactions and the equilibrium constants for the interactions with ethanol differ among the four phases. For example, the interactions of small organic ligands with the liquid-crystalline L_{α} phase has traditionally been treated as a nonspecific partitioning between the aqueous phase and the lipid phase, similar to the octanol–water partitioning of these solutes (Seeman, 1972; Hill, 1974; Lee, 1977; Rowe, 1983). This is consistent with the linear nature of the low concentration effect on the transition temperature for the main transition (insets to Figure 11). On the other hand, the mechanism of interaction of ethanol with the interdigitated gel phase is better described by a model involving specific binding to a finite number of sites in the interfacial region, as is suggested by the hyperbolic shape of the high alcohol region of the T_m dependence on ethanol (Rowe, 1983). The preferential interactions of ethanol with $L_{\beta}I$ compared to P_{β}' are indicated by the changes in slope in both the upper and lower curves of Figure 11 at the ethanol concentration where the P_{β}' phase is replaced by the $L_{\beta}I$ phase. These preferential interactions are probably due to a larger number of hydrophobic sites in $L_{\beta}I$ compared to P_{β}' due to the presence of the terminal methyls from the opposite side of the lamella in the interfacial region. In the case of the relative interactions of ethanol with P_{β}' and L_{β}', as indicated by the effect of ethanol on the L_{β}' to P_{β}' transition (Veiro et al., 1987), the rippling of the interfacial region in the P_{β}' may expose some more hydrophobic sites than are available in the L_{β}'.

Chain Length Effects. Comparison of the results obtained for DPPC and DSPC shows that the results are generally similar for these two chain length lipids. However, as seen in both Figures 10 and 11, the threshold ethanol concentration for conversion of P_{β}' to $L_{\beta}I$ is lower for the longer chain lipid. This is consistent with the acyl chain length dependence of the biphasic effect on the main transition (Rowe, 1983), in which it was shown that the longer the lipid chain length, the lower the concentration of ethanol needed to induce the biphasic effect. The biphasic effect is a reflection of the conversion of P_{β}' to $L_{\beta}I$. Thus, it appears that additional carbons stabilize the $L_{\beta}I$ phase relative to the P_{β}' phase. An unresolved issue in the previous study (Rowe, 1983) was whether the chain length dependence of the threshold of the biphasic effect was due to chain length itself or to the temperature effect of measuring each biphasic effect at a different temperature (i.e., the respective main transition temperature for each lipid). The finding that the P_{β}' to $L_{\beta}I$ transition is not temperature dependent shows that the variation in threshold concentrations reported previously (Rowe, 1983) is a chain length effect rather than a temperature effect. This result supports the analysis of the chain length effect by Simon et al. (1986), which suggested that the additional methylene groups stabilize $L_{\beta}I$ relative to the noninterdigitated gel because the acyl chain region has closer van der Waals' contacts in the interdigitated phase than in the noninterdigitated phase.

Conclusion

Our results demonstrate that there is a delicate balance of forces which determine whether or not a PC will be interdigitated in the gel phase. In addition to the variety of solvent conditions which induce interdigitation, we have now shown that temperature is also an important variable. The delicate balance of forces which determines the phase behavior of these lipids is further demonstrated by comparison of the results reported here with the behavior of two related PC's, which vary in the linkages of their hydrocarbon chains to the glycerol.

The ether-linked analogue of DPPC, dihexadecylphosphatidylcholine (DHPC), has recently been shown to exist in the interdigitated phase in the absence of any additives (Ruocco et al., 1985). As it is heated, it goes from the interdigitated $L_{\beta}I$ to the noninterdigitated P_{β}' before melting to the L_{α} phase (Laggner et al., 1987; Kim et al., 1987). This is in contrast to DPPC (in the presence of ethanol) which goes from a noninterdigitated phase to an interdigitated phase with increasing temperature. A recent study on the effects of ethanol on the DHPC transitions shows that ethanol interacts preferentially with the $L_{\beta}I$ phase in this lipid as it does in DPPC (Veiro et al., 1988).

The $L_{\beta}I$ phase has also been observed in β-DPPC at temperatures between 30 and 35 °C in the absence of any additives (Serrallach et al., 1983). At lower temperature it exists in a noninterdigitated subgel phase, and upon heating it goes to the $L_{\beta}I$ phase. At 37 °C it then melts to the L_{α} phase. Thus, it is similar to DPPC (in the presence of ethanol) in that it goes from a noninterdigitated phase to an interdigitated phase with increasing temperature. This system also exhibits hysteresis and/or irreversibility of some of its transitions. For this lipid it was suggested that the glycerol backbone adopts an orientation parallel to the bilayer surface, resulting in packing differences in the acyl chains as well as the interfacial region, compared to DPPC, which leads to the thermodynamic differences between these positional isomers (Serrallach et al., 1983).

Acknowledgments

We thank Dr. Kenneth Audus of the Department of Pharmaceutical Chemistry of the University of Kansas, Lawrence, KS, for performing fluorescence lifetime measurements. We also thank Dr. Sidney Simon, Duke University Medical Center, for helpful comments.

Registry No. DPPC, 2644-64-6; DSPC, 4539-70-2; DPH, 1720-32-7; ethanol, 64-17-5.

References

Barrow, D. A., & Lentz, B. R. (1985) *Biophys. J. 48*, 221–234.

Boggs, J. M., & Rangaraj, G. (1985) *Biochim. Biophys. Acta 816*, 221–233.

Boggs, J. M., Rangaraj, G., & Koshy, K. M. (1986) *Chem. Phys. Lipids 40*, 23–34.

Braganza, L. F., & Worcester, D. L. (1986) *Biochemistry 25*, 2591–2596.

Cunningham, B. A., & Lis, L. J. (1986) *Biochim. Biophys. Acta 861*, 237–242.

Davenport, L., Dale, R. E., Bisby, R. H., & Cundall, R. H. (1985) *Biochemistry 24*, 4097–4108.

Herold, L. H., Rowe, E. S., & Khalifah, R. G. (1987) *Chem. Phys. Lipids 43*, 215–226.

Hill, M. W. (1974) *Biochim. Biophys. Acta 356*, 117–124.

Huang, C., Mason, J. T., & Levin, I. W. (1983) *Biochemistry 22*, 2775–2780.

Hui, S. W., & Huang, C.-H. (1986) *Biochemistry 25*, 1330–1335.

Hui, S. W., Mason, J. T., & Huang, C. (1984) *Biochemistry 23*, 5570–5577.

Janiak, M. J., Small, D. M., & Shipley, G. G. (1976) *Biochemistry 15*, 4575–4580.

Janiak, M. J., Small, D. M., & Shipley, G. G. (1979) *J. Biol. Chem. 254*, 6068–6078.

Kamaya, H., Kaneshina, S., & Ueda, I. (1981) *Biochim. Biophys. Acta 646*, 135–142.

Kim, J. T., Mattai, J., & Shipley, G. G. (1987) *Biochemistry 26*, 6592-6598.
Laggner, P., Lohner, K., Degovics, G., Muller, K., & Schuster, A. (1987) *Chem. Phys. Lipids 44*, 31-60.
Lakowicz, J. R. (1983) *Principles of Fluorescence Spectroscopy*, Plenum, New York.
Lee, A. G. (1977) *Biochim. Biophys. Acta 472*, 285-344.
Lentz, B. R., Barenholz, Y., & Thompson, T. E. (1976) *Biochemistry 15*, 4521-4528.
Mattai, J., Sripada, P. K., & Shipley, G. G. (1987) *Biochemistry 26*, 3287-3297.
McDaniel, R. V., McIntosh, T. J., & Simon, S. A. (1983) *Biochim. Biophys. Acta 731*, 97-108.
McIntosh, T. J. (1978) *Biochim. Biophys. Acta 649*, 325-335.
McIntosh, T. J. (1980) *Biophys. J. 29*, 237-246.
McIntosh, T. J., McDaniel, R. V., & Simon, S. A. (1983) *Biochim. Biophys. Acta 731*, 109-114.
McIntosh, T. J., Simon, S. A., Ellington, J. C., & Porter, N. A. (1984) *Biochemistry 23*, 4038-4044.
O'Leary, T. J., & Levin, I. W. (1984) *Biochim. Biophys. Acta 776*, 185-189.
Ranck, J. L., Keira, R., & Luzzati, V. (1977) *Biochim. Biophys. Acta 488*, 432-441.
Rowe, E. S. (1983) *Biochemistry 22*, 3299-3305.
Rowe, E. S. (1985) *Biochim. Biophys. Acta 813*, 321-330.
Rowe, E. S. (1987) *Biochemistry 26*, 46-51.
Rowe, E. S., Fernandes, A., & Khalifah, R. G. (1987a) *Biochim. Biophys. Acta 905*, 151-161.
Rowe, E. S., Veiro, J. A., Nambi, P., & Herold, L. L. (1987b) *Biophys. J. 51*, 238a.
Ruocco, M. J., Siminovitch, D. J., & Griffin, R. G. (1985) *Biochemistry 24*, 2406-2411.
Seeman, P. (1972) *Pharmacol. Rev. 24*, 583-654.
Serrallach, E. N., Dijkman, R., De Haas, G. H., & Shipley, G. G. (1983) *J. Mol. Biol. 170*, 155-174.
Simon, S. A., & McIntosh, T. J. (1984) *Biochim. Biophys. Acta 773*, 169-172.
Simon, S. A., McIntosh, T. J., & Hines, M. L. (1986) *Molecular and Cellular Mechanisms of Anesthetics* (Roth, S. H., & Miller, K. W., Eds.) pp 297-308, Plenum, New York.
Stamatoff, J., Feuer, B., Guggenheim, H. J., Tellez, G., & Yamane, T. (1982) *Biophys. J. 38*, 217-226.
Tardieu, A., Luzzati, V., & Reman, R. C. (1973) *J. Mol. Biol. 75*, 711-733.
Veiro, J. A., Nambi, P., Herold, L. L., & Rowe, E. S. (1987) *Biochim. Biophys. Acta 900*, 230-238.
Veiro, J. A., Nambi, P., & Rowe, E. S. (1988) *Biochim. Biophys. Acta 943*, 108-111.
Weber, G. (1981) *J. Phys. Chem. 85*, 949.
Xu, H., & Huang, C.-H. (1987) *Biochemistry 26*, 1036-1043.

Tropomyosin Inhibits the Rate of Actin Polymerization by Stabilizing Actin Filaments†

Sarah E. Hitchcock-DeGregori*
Department of Anatomy, UMDNJ-Robert Wood Johnson Medical School, Piscataway, New Jersey 08854
Prakash Sampath and Thomas D. Pollard
Department of Cell Biology and Anatomy, Johns Hopkins Medical School, Baltimore, Maryland 21205
Received July 6, 1988

ABSTRACT: Tropomyosin inhibition of the rate of spontaneous polymerization of actin is associated with binding of tropomyosin to actin filaments. Rate constants determined by using a direct electron microscopic assay of elongation showed that $\alpha\alpha$- and $\alpha\beta$-tropomyosin have a small or no effect on the rate of elongation at either end of the filaments. The most likely explanation for the inhibition of the rate of polymerization of actin in bulk samples is that tropomyosin reduces the number of filament ends by mechanical stabilization of the filaments.

The dynamics of actin polymerization and filament organization are affected by different types of actin binding proteins (Korn, 1982; Frieden, 1985; Pollard & Cooper, 1986). Tropomyosin interests us because it binds along the length of actin filaments and might have a role in length determination of thin filaments. Its role in the regulation of striated muscle contraction is well established (Leavis & Gergely, 1984; El Saleh et al., 1986). Though tropomyosin is present in most animal cells, the isoforms are different, and the functional significance of various isoforms is unknown (Côté, 1983).

Tropomyosin inhibits the rate of actin polymerization without altering the critical concentration (Pragay & Gergely, 1968; Wegner, 1982a; Hitchcock-DeGregori & Maris, 1983; Lal & Korn, 1986). Tropomyosin could affect the number of filaments (Wegner, 1982b; Wegner & Savko, 1982) and/or the rate at which each filament elongates. Wegner (1982b) reported that the kinetics of inhibition of polymerization could be explained by stabilization of actin against fragmentation, but in the absence of direct determination of the number of filament ends, he could not rule out an effect on elongation. Lal and Korn (1986) also reported inhibition of polymerization by tropomyosin but suggested that reduced rates of association and dissociation of subunits from the ends of filaments contributed to the overall effect.

We carried out similar experiments showing that inhibition of polymerization was associated with binding of tropomyosin to F-actin (Hitchcock-DeGregori & Maris, 1983). Since the inhibition was not overcome by addition of F-actin nuclei, we suggested that tropomyosin may inhibit elongation as well as

† Supported by NIH Grants GM36326 to S.E.H. and GM26338 to T.D.P. and by Research Career Development Award AM01637 to S. E.H.
* Address correspondence to this author.

0006-2960/88/0427-9182$01.50/0